

Molecular Dynamics Investigation of the Effects of Concentration on Hydrogen Bonding in Aqueous Solutions of Methanol, Ethylene Glycol and Glycerol

Ning Zhang, Weizhong Li,* Cong Chen, Jianguo Zuo, and Lindong Weng

Key Laboratory of Ocean Energy Utilization and Energy Conservation of Ministry of Education,
Dalian University of Technology, Dalian 116024, China. *E-mail: wzhongli@dlut.edu.cn
Received April 13, 2013, Accepted June 20, 2013

Hydrogen bonding interaction between alcohols and water molecules is an important characteristic in the aqueous solutions of alcohols. In this paper, a series of molecular dynamics simulations have been performed to investigate the aqueous solutions of low molecular weight alcohols (methanol, ethylene glycol and glycerol) at the concentrations covering a broad range from 1 to 90 mol %. The work focuses on studying the effect of the alcohols molecules on the hydrogen bonding of water molecules in binary mixtures. By analyzing the hydrogen bonding ability of the hydroxyl (-OH) groups for the three alcohols, it is found that the hydroxyl group of methanol prefers to form more hydrogen bonds than that of ethylene glycol and glycerol due to the intra- and intermolecular effects. It is also shown that concentration has significant effect on the ability of alcohol molecule to hydrogen bond water molecules. Understanding the hydrogen bonding characteristics of the aqueous solutions is helpful to reveal the cryoprotective mechanisms of methanol, ethylene glycol and glycerol in aqueous solutions.

Key Words : Molecular dynamics simulation, Methanol, Ethylene glycol, Glycerol, Hydrogen bond

Introduction

Cryopreservation is an effective method for the long-term storage of living cells or tissues at low temperature, so that it is widely used in the fields of medicine,¹ food,² biological industry,³ etc. For the purpose of effective long-term storage, some amphiphilic substances called cryoprotective agent (CPA), including relatively small alcohol molecules, like methanol (MET), ethylene glycol (EG) and glycerol (GLY), are employed to protect cells against freezing damage. In the freezing process of cryopreservation, the volume of cell decreases with time mainly due to intracellular water loss.⁴⁻⁶ The removal of cell water is a critical part of the intracellular water, and the remaining water inside the cell can be categorized into two parts: the water participating in intracellular ice formation and intracellular ice growth, and the water bounded by CPAs and cytoplasmic molecules through hydrogen bonds (H-bonds) or other interactions.

Investigations on intracellular water have been implemented by cryobiologists both theoretically and experimentally. The model proposed by Jacobs⁵ in 1933 could predict the water loss from cell with time, subject to certain simplifying assumptions. After that, a model was introduced by Mazur and colleagues⁴ to further describe the water loss subjected to temperature. Kedem and Katchalsky⁶ developed a formalism to describe osmotic transport across cell membrane with the consideration of coupled cotransport of water and solute. Several experimental investigations⁷ also have been employed to measure the volumetric response of cells during freezing. Besides, there have been amounts of studies⁸⁻¹¹ on intracellular ice formation and growth. However, there is less investigation on the intracellular water (bound water)

restricted by solute like CPAs and cytoplasmic molecules.

Although the content of bound water is marginal and always neglected in the abovementioned models, it nevertheless is responsible for many biological processes and its inherent formation mechanisms have yet to be fully understood.¹²⁻¹⁴ Molecular dynamics (MD) simulation provides researchers with a novel approach to explore the microscopic behavior and structure at atomistic level, which may enable the determination of bound water content and the exploration of molecular mechanisms of its formation. There have been numerous MD simulations on the interaction of water and CPA molecules, complementary to experiments.

In the early years, Lovelock¹⁵ tested the protective action of fifteen neutral solutes, including all the alcohols mentioned above, against the haemolysis of human red blood cells, and developed the theory of the colligative action of CPA. In recent years, the summary of the experimental research on various CPAs was provided by Zdenek¹⁶ shows that each CPA has its advantage in specific applications. It was also found that the hydrophilic groups make a significant effect on the cryopreservation. Later, Towey and colleagues¹⁷ investigated the structure of the pure cryoprotectant GLY in the liquid state using Neutron diffraction, aiming at evaluating the conformation and H-bonding properties of pure liquid GLY. Alexander and Tatyana¹⁸ conducted the MD simulation to study the effect of aqueous mixtures of cryoprotective solutes such as EG and GLY on lipid membrane. It has been found that the concentration of the CPA solutes is a vital factor to the membrane damage. Dashnau and colleagues¹⁹ determined the H-bonding patterns of GLY and its mixtures with water by both experimental and MD simulation methods, which gave the accordant results of the

effect of the concentration on the H-bonding structure. Cong Chen *et al.*²⁰ conducted a series of MD simulations of GLY aqueous solution to investigate the mechanism of H-bonding interaction between GLY and water. After that, H-bonding characteristics of cryoprotective media (glycerol/sodium chloride/water mixtures) were investigated in depth.²¹ Weng and his colleagues²² quantitatively investigated the relationship between hydrogen bonded water and the concentration of EG and GLY aqueous solutions, and we²³ also used Perkin-Elmer Diamond Differential Scanning Calorimetry (DSC) to verify the simulation findings.

Hydrogen bonding (H-bonding) is one of the most important forms of non-bonded interaction in water and its mixtures. Some anomalies of supercooled water are well explained by analyzing the character of H-bonding.²⁴ In the aqueous solution of CPA, H-bonds are usually weak compared to covalent bonds, however, H-bonds are so numerous as to play a vital role in the intermolecular interaction. MET, EG and GLY are the commonly used CPAs for the properties of protection against dehydration, freezing point depression and ice nucleation inhibition in the long-term cryopreservation. These alcohol molecules are preferable to form H-bonds and permeable to membrane, and the permeated alcohol molecules hydrogen bond to water molecules. The solute-solvent hydrogen bonding interaction can inhibit the intracellular ice formation. High intracellular concentration also leads to cell injury during cryopreservation. Thus it is significant to control the proportion of the intracellular water hydrogen bonded to CPA molecules. However, the current research situation is still at the exploratory stage. Specifically, the intrinsic interaction mechanisms of CPAs in cell sap have been being debated for decades. Therefore, research on the effect of concentration on the H-bonding property in the CPA aqueous solution becomes the target of this paper.

The present work is an MD simulation study focusing on aqueous solutions of three linearly saturated alcohols including MET, EG and GLY, of which each carbon atom is conjunct with one hydroxyl group. In this paper, a series of MD simulations were carried out to investigate the effect of concentration on the H-bonding interaction between alcohol and water in their binary mixtures. In addition, we present the simulated densities of the solutions with different concentrations along with the corresponding experimental results for comparison. To the best of our knowledge, although there are numerous studies on alcohol aqueous solution, the characteristics of hydration or hydrogen bonding have not been fully understood. Studies^{18-20,25-27} on dilute solutions provide significant results of the hydrogen bonding characteristics of dilute solutions, which are insufficient to exactly reflect the solutions in a broad concentration range. Herein, the investigation on the aqueous solutions of MET, EG and GLY almost covers the whole concentration range by certain concentration increments, helpful to exactly describe the variation of H-bonding characteristics with concentration. The results of our qualitative and quantitative analysis of the concentration effect on H-bonding network are presented in this paper in order to broaden and deepen the understanding

of the microscopic mechanisms of cryoprotective ability of the three alcohol solutes in the aqueous environment.

Model and Methodology

Simulation Details. In this work, MD simulations were implemented by virtue of the MD simulation package NAMD²⁸ (version 2.7) using the all-atom empirical CHARMM22 force field. The transferable intermolecular potential 3 point (TIP3P) water model²⁹ was employed as solvent in the present study. The models of MET,³⁰ EG and GLY³¹ from the previous studies were used as solutes which are mixed with water in varying proportions. For each system, the total amount of molecules are maintained constant at 1,000. As the number of molecules was constant, the volume of the systems would gradually expand with the increasing concentration. The simulation systems were constructed with desired combinations. A box with a specified number of alcohol solutes was generated, and then a specified number of water molecules were added into the box. One system of CPA aqueous solution with desired concentration of alcohols was then obtained. Furthermore, the simulation boxes were always set to be cubic, avoiding the effect of different boundary sizes. Alcohol molecules were uniformly distributed in the water boxes in order to reduce the mixing time of the alcohol clusters.¹⁸ After completing the system construction, a short time of 2 ps was conducted to minimize the energy of the binary mixture and then a run for 4.0 ns was carried out to fully equilibrate the system.

In the simulation, the temperature and pressure were maintained at about 298 K and 1.0 bar, namely the isothermal-isobaric (NpT) ensemble. Periodic boundary conditions were used in three dimensions to eliminate edge effect. Langevin dynamics and Langevin piston Nosé-Hoover methods³² were employed to control the temperature and pressure, respectively. Full electrostatic interaction was solved using the particle mesh Ewald (PME) method³³ with the grid spacing of about 1.0 Å. The parameter cutoff was set to 12 Å, which specified the distance at which van der Waals interaction was truncated and the long and short range forces were separated for electrostatic interactions. With this scheme, all the van der Waals interactions were ignored beyond the specified distance, or assumed to be zero. As a result, the computational cost was greatly reduced. In order to bring the non-bonded potentials smoothly to zero at the cutoff distance, the switching function and the shifting function were applied to van der Waals potential and electrostatics potential, respectively. The bond between hydrogen and its "mother atom" was constrained to the nominal length. The SHAKE algorithm³⁴ was used to fulfill the constraint. During the simulation run, data was sampled every 1000 time steps, namely 2.0 ps. Each system was first equilibrated for 4.0 ns, and then additional run for 1.0 ns was performed for analysis with a time step of 2.0 fs.

Long simulation run guarantees the simulated system in complete equilibrium situation. The properties of total, potential and kinetic energies reflect the stability of the

system. In the present study, the values of the total, potential and kinetic energies of the system exhibit small fluctuation around certain values after about 2 ns. To illustrate this, the values of the total, potential and kinetic energies of the 90 mol % GLY aqueous solution as a function of the simulation time are depicted as an example in the Supporting Information.

Definition of H-bonds. Geometric³⁵ and energetic³⁶ criteria are two widely used methods to determine the existence of H-bond. In the present study, we employed the geometric criterion, which is widely used by researchers³⁷⁻⁴⁰ for its effectiveness and conveniences. In the present work, H-bonds exist in the forms of the strong O-H...O and the weak C-H...O. It has been proved that the O-H...O H-bonds take the dominant place in the alcohol aqueous solution, while the C-H...O H-bonds have much fewer opportunities to appear in the solutions due to its weak interaction.²⁶ Furthermore, the C-H...O interaction is referred to as special H-bond and attributed to a few interactions.⁴¹⁻⁴³ Thus further investigations need to be carried out on the C-H...O interaction. For the two reasons, only the O-H...O interactions are taken into account in this paper.

The geometry of the definition for one H-bond O-H...O involves the distance O...O, the H-bond length O...H, the O-H...O H-bond angle, the H-O...O angle, and the O...O...H angle. The symbol “—” stands for the covalent bond, and the symbol “...” represents non-bonded interaction. All the commonly used geometric criteria are defined with three or two of the abovementioned geometric parameters. The geometric criterion used here can be expressed as follows:

- (1) The distance R_{oo} between the donor and the acceptor is less than the threshold value R_{oo}^c ,
- (2) The distance R_{OH} between the acceptor and the hydrogen of the donor is less than R_{OH}^c ,
- (3) The H-O...O angle φ is less than φ^c .

The threshold values of distance are often determined by the radial distribution functions (RDFs). Thus the RDFs $g_{OH}(r)$ and $g_{OO}(r)$ are needed to determine the threshold values of distance. The positions of the first minima are chosen as the cutoff distances R_{oo}^c and R_{OH}^c . RDFs of the O_{water}-O_{alcohol} pair for MET, EG and GLY aqueous solutions are presented in Figure 1, for brevity, other RDFs (including O_{water}-O_{water}, O_{water}-H_{water}, O_{alcohol}-H_{water}, O_{water}-H_{alcohol}, O_{alcohol}-O_{alcohol} and O_{alcohol}-H_{alcohol}) are not shown in this paper. It is shown in Figure 1 that the width of the first trough varies with concentration, but the first minimum position is kept at around 3.5 Å. In all cases, the first minimum positions of water-water site-site partial RDFs for the pairs O_{water}-O_{water} shift to a short distance from 3.5 to 3.7 Å, but the first minimum positions for the oxygen-hydrogen pairs of the water molecule is unchanged at 2.45 Å. This phenomenon is consistent with the neutron diffraction experimental results.^{44,45} In order to investigate the effect of the shifted O_{water}-O_{water} distance on hydrogen bonding, we determined the water-water H-bonds with two criteria: 2.45 Å as the cutoff distance R_{OH}^c , and 3.5 and 3.7 Å for R_{oo}^c , respectively. The two geometric criteria produced similar

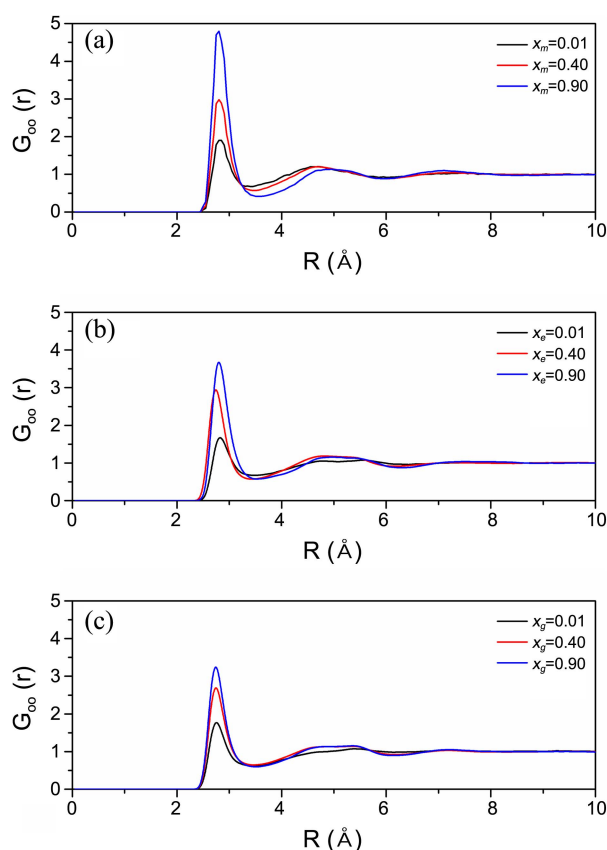


Figure 1. Alcohol-water partial RDFs for the alcohol oxygen-water oxygen pairings in the aqueous solutions of MET (a), EG (b) and GLY (c). The molar fractions of the mixtures for each RDF are shown in the figure.

results for the amount of the water-water H-bonds. Besides, the first minimum positions of water-alcohol partial RDFs for the oxygen-hydrogen pairs O_{water}-H_{alcohol} and O_{alcohol}-H_{water} maintain unchanged at 2.45 Å. For all the alcohol-alcohol RDFs of the O_{alcohol}-O_{alcohol} and O_{alcohol}-H_{alcohol} pairs, the minimum positions maintain at 3.5 and 2.6 Å, respectively. This is consistent with the simulation results by Padró *et al.*²⁵ Therefore, the same cut-off distances for the alcohol-water and water-water H-bonds were used with the values $R_{oo}^c = 3.5$ Å and $R_{OH}^c = 2.45$ Å; the cut-off distances for the alcohol-alcohol H-bonds were selected as $R_{oo}^c = 3.5$ Å and $R_{OH}^c = 2.6$ Å. The angular cutoff is chosen to be a widely accepted value $\varphi^c = 30^\circ$.^{25,46}

Results and Discussion

Density of the Binary Mixtures. MET/EG/GLY and water are mixed in varying combinations ranging from 1-90 mol %. The simulated densities of dilute solutions of EG and GLY were shown in our previous investigations,²² which presented the simulated density of mixture in well agreement with the experiment. Here the simulated densities of MET solutions are tabulated in Table 1 together with the experimental densities for comparison. The results for EG and GLY aqueous solutions are listed in the Supporting

Table 1. The concentration of MET aqueous solution and the comparison of the simulation and the experimental results. “mol %” and “wt %” denote the percentage of mole fraction and mass fraction of the aqueous solutions, respectively

mol %	wt %	ρ_{sim} (g/L)	ρ_{exp} (g/L) ^a	$(\rho_{\text{sim}} - \rho_{\text{exp}}) / \rho_{\text{exp}} \times 100\%$
1	2	1005.5 ± 8.5	994.1	1.15
5	9	986.1 ± 8.2	982.2	0.39
10	16	965.6 ± 7.9	971.2	-0.58
20	31	929.6 ± 7.6	947.5	-1.89
30	43	900.2 ± 7.3	925.9	-2.78
40	54	876.0 ± 6.9	903.8	-3.08
60	73	835.4 ± 6.8	859.9	-2.85
80	88	800.7 ± 6.6	821.7	-2.56
90	94	784.2 ± 6.2	804.5	-2.52

^aThe experimental densities of the mixtures of MET and water refer to the reference.⁴⁷

Information. The simulated density is obtained by averaging the volumes of the simulation box over a relatively long time that would reduce the fluctuation effect. It is noted that the relative error of the simulation result is no more than 5% which lies in acceptable range. The maximum absolute relative error with the value 3.08 % occurs in the solution of 40 mol %. The density of the mixture of water with EG or GLY has an increasing tendency with the increase of concentration, as shown in the Supporting Information.

Evaluation of H-bonding Ability of MET, EG and GLY in Aqueous Solution.

H-bonding Analysis of Hydroxyl Groups on MET, EG and GLY: In this section, the H-bonding ability of MET, EG and GLY in aqueous solution will be evaluated by means of the statistics of H-bonds formed by three types including solute-solute (S-S), water-solute (W-S) and water-water (W-W) H-bonds. Figure 2 shows the average number of H-bonds per hydroxyl group $\langle n(\text{HB})_{\text{OH}} \rangle$ as a function of the concentration of MET, EG and GLY. It is shown that the hydroxyl group of MET favors to form more H-bonds compared with EG and GLY. With the same weight, MET would exhibit greater H-bonding ability than the other two alcohols. In water-rich region, the value of $\langle n(\text{HB})_{\text{OH}} \rangle$ for EG is closer to GLY than to MET. In the middle concentration range (30-70 wt %), difference of $\langle n(\text{HB})_{\text{OH}} \rangle$ between MET and EG is similar to that between EG and GLY. In alcohol-rich region, the values of $\langle n(\text{HB})_{\text{OH}} \rangle$ for the three alcohols decrease with the rising concentration and approach to the same value, similar to the findings⁴⁸ that the mean number of H-bonds per molecule in pure liquid system is proportional to the number of hydroxyl groups per molecule. Besides, $\langle n(\text{HB})_{\text{OH}} \rangle$ shows gradual descent in the low-middle concentrated region and then the decreasing tendency becomes sharper, especially for the EG and GLY solutions. In detail, the values of $\langle n(\text{HB})_{\text{OH}} \rangle$ for MET, EG and GLY solutions grow by 11.1, 3.2 and 6.2% within the concentration approximately from 2 to 30 wt %; and in the range of the concentration from 70 to 95 wt %, the three corre-

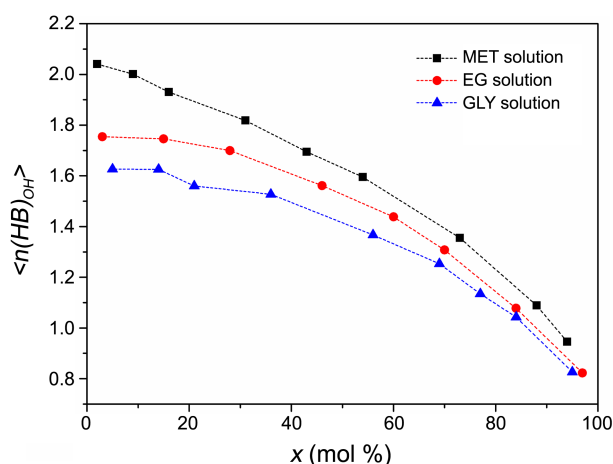


Figure 2. The average number of H-bonds per hydroxyl group of MET, EG and GLY in the binary mixtures. $\langle \dots \rangle$ denotes the ensemble average value of $n(\text{HB})_{\text{OH}}$. The mass fraction of alcohol solutes in the aqueous solution is used to define the concentration.

sponding values grow much sharper by 30.8, 38.3 and 34.5%, respectively.

On one hand, the decrease of $\langle n(\text{HB})_{\text{OH}} \rangle$ is ascribed to the increase of the S-S H-bonds. The statistical method for the S-S H-bonds is non-weighted, which means that the contribution of one S-S H-bond is as same as that of one W-S H-bond to the total amount of H-bonds formed by alcohol. Therefore, with the concentration increases, the increasing S-S H-bonds gradually overtake the decreasing W-S H-bonds, resulting in the decrease of the value of $\langle n(\text{HB})_{\text{OH}} \rangle$. On the other hand, the molecular size is another reason for the decreasing amount of H-bonds formed by alcohol with increasing the concentration. The three alcohol molecules are all larger than water molecule in size. In dilute solution, each alcohol molecule is nearly surrounded by small water molecules. With the addition of alcohol, the surrounded water molecules are gradually replaced by the larger alcohol molecules, and the amount of the molecules surrounding one alcohol molecule would decrease due to the spatial limit. Therefore, with the concentration increases, the amount of H-bonds formed by alcohol is reduced by the intermolecular effect resulting from the molecular size.

It is shown in Figure 2 that the value of $\langle n(\text{HB})_{\text{OH}} \rangle$ for MET is obviously larger than those for EG and GLY in the dilute solutions. At low concentration, the probability of the S-S H-bonding interaction is very low and the H-bonds formed by alcohol solute mainly exist in the W-S form. Thus it indicates that the hydroxyl group of MET has greater ability to form H-bond with water than that of EG and GLY.

To explain the differences of $\langle n(\text{HB})_{\text{OH}} \rangle$ between MET, EG and GLY in Figure 2, attention should be paid on the hydroxyl group content of the alcohol molecule: 1 in MET, 2 in EG and 3 in GLY. Taking the GLY molecules for example, in the viewpoint of intramolecular interaction, the three hydroxyl groups are very close to each other, and each hydroxyl group has more or less effect on the H-bonding of its neighbor Hydroxyl groups. Figure 3 presents the mean

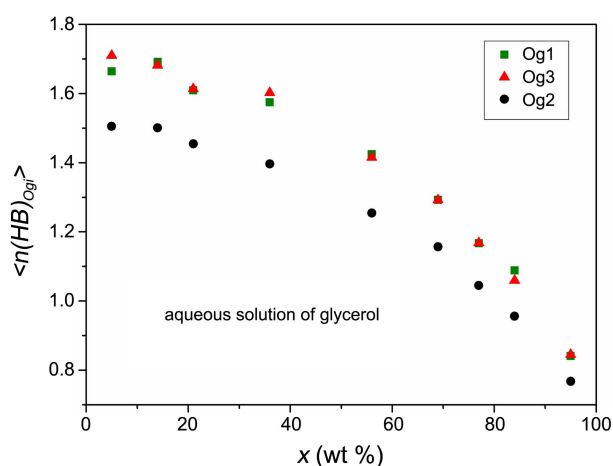


Figure 3. The mean numbers of H-bonds per hydroxyl group are plotted in scattered points (full squared, circular and triangle) for the three types of hydroxyl groups, respectively. Og1 and Og3 denote the hydroxyl groups on the two sides of the glycerol molecules; Og2 denotes the middle hydroxyl groups of the glycerol molecules.

numbers of H-bonds formed by the three hydroxyl groups in the GLY molecule $\langle n(HB)_{Ogi} \rangle$. The value of $\langle n(HB)_{Og2} \rangle$ is obviously less than the other two, while the two side hydroxyl groups form similar amount of H-bonds. The middle hydroxyl group has more intramolecular effect due to the fact that there are two neighbor hydroxyl groups next to it. As for the EG molecule, its hydroxyl groups only have one neighbor similar to that of the two side hydroxyl groups of GLY, resulting in less effect on the amount of H-bonds per hydroxyl group for EG molecules. The hydroxyl group in the MET molecule has no neighbor hydroxyl group, thus the value of $\langle n(HB)_{OH} \rangle$ for MET should be the largest among the three alcohols in the aqueous environment without the effect of the intramolecular hydroxyl group. The value of $\langle n(HB)_{OH} \rangle$ may also be influenced by the charge of the oxygen atoms of the hydroxyl groups, however, the oxygen atoms of the hydroxyl groups have the same charge in the models of MET, EG and GLY.

Therefore, it can be concluded that the order of the ability to form H-bonds or W-S H-bonds for the hydroxyl groups of the three alcohols is MET > EG > GLY due to the intra- and intermolecular effects. However, the concentration effects on the H-bonding ability of the hydroxyl group decrease with increasing the proportion of alcohol in the aqueous solution. Other investigations such as Monte Carlo and ab-initio quantum mechanical calculations could give the verifications of the conclusion from the perspective of energy.

Average H-bonding of MET, EG and GLY in the Aqueous Mixtures: The amount of H-bonds per hydroxyl group for GLY is less than MET and EG, however, GLY has the largest ability to form H-bonds due to its high hydroxyl group content per molecule. It is also shown in Figure 4 that the average number of W-S H-bonds per alcohol solute for MET, EG and GLY decreases with the concentration increases, while there is a contrary change trend for S-S H-bonds. At low concentrations, the value of $\langle n_{HB} \rangle$ for the W-S H-bonds

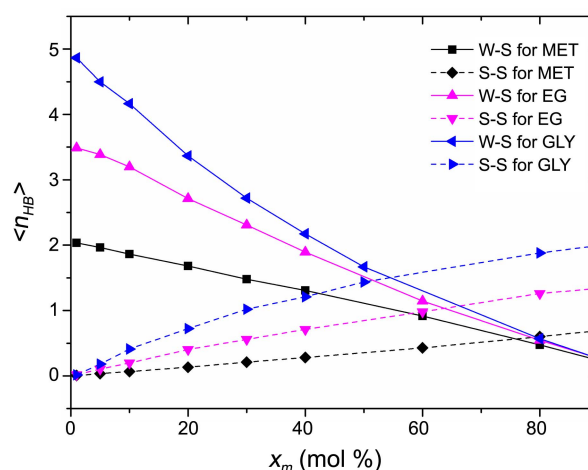


Figure 4. Average number of H-bonds per alcohol molecule ($\langle n_{HB} \rangle$) for MET, EG or GLY. The total n_{HB} is separated into two contributions of W-S and S-S H-bonds.

predominate the total average number of H-bonds formed by solute due to the preferential solvation effect of water. The S-S H-bonds compensate for the decreasing W-S H-bonds with the concentration increases. In comparison, the variations of the W-S H-bonds per alcohol molecule are larger than the S-S H-bonds variations as the mole fraction goes from 0.01 to 0.90. It is the reason why the average numbers of H-bonds per hydroxyl group goes down rapidly with the concentration increases as shown in Figure 2.

In the entire concentration range, GLY has the largest values of $\langle n_{HB} \rangle$ for the W-S and S-S H-bonds. It indicates that GLY molecule is more active to H-bond water molecules than MET and EG molecules. However, the predominance of $\langle n_{HB} \rangle$ of the W-S H-bonds for GLY decreases with the concentration increases, obviously resulting from the decreasing water molecules. For the concentrations lower than 40 mol %, the $\langle n_{HB} \rangle$ values of GLY for the W-S and S-S H-bonds change greater than those at the higher concentration. The solvation of the alcohol molecule is enhanced by its dilution in water. As shown in Figure 4, the average numbers of the W-S H-bonds per alcohol molecule for MET, EG and GLY decrease from 2.04, 3.49 and 4.86 to 0.24, 0.27 and 0.27 from 1 to 90 mol %, respectively. This phenomenon is similar to that of ethanol in its aqueous mixture.⁴⁰

Effect of Concentration on the H-bonding Ability of “Bound Water”. For cryopreservation, the alcohols (*i.e.* MET, EG and GLY) have been widely used as CPA because of the advantage of suppressing the formation of ice crystallization. The W-W H-bonds provide the potential for the formation of intracellular ice crystallization, while the W-S H-bonds can suppress the ice crystallization. In our previous study,²² we defined one water molecule with one or more W-S H-bonds as “bound water” and evaluated the ability of the alcohol molecules to form H-bonds with water molecules by two criteria: the number of “bound water” by one solute molecule N_{bw}/N_s and the mass fraction of “bound water” out of the total water W_{bw}/W_w . Here, a further investigation on MET, EG and GLY solutions in a broader

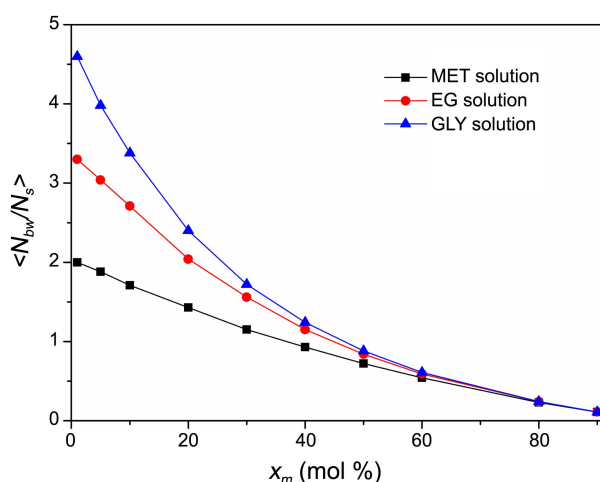


Figure 5. “Bound water” content per solute molecule N_{bw}/N_s for MET, EG and GLY aqueous solutions as a functions of solute mole fraction at 298 K (The lines just guide to the eyes). $\langle \dots \rangle$ denotes the ensemble average of the value in the bracket. N_{bw} is the number of the “bound water”, and N_s is the number of the alcohol solute in the aqueous solution.

range of concentration is made as shown in Figure 5. In this study, mole fraction of solute is used to quantify the concentration, which could exhibit much clearer picture in the broad range of concentration than the previously used molality for concentration.²²

The results presented in Figure 5 show the similar findings with our previously study²² that N_{bw}/N_s decreases with increasing the concentration. The results for GLY shows sharper change than the other two curves due to the fact that the GLY molecule is a trihydric alcohol, which results in more hydrogen bonded water molecules in the solution. Besides, the values of N_{bw}/N_s present nonlinear change with concentration, inconsistent with our proposed linear change tendency. This is due to the fact that alcohol molecules get more interested in the formation of the S-S H-bonds as the solution becomes more concentrated. It is shown in Figure 4 that the average number of W-S H-bonds per alcohol molecule decreases as the alcohol mole fraction increases. As a result of the reduced contribution of the added alcohol molecules to the formation of the W-S H-bonds, the decreasing tendency of N_{bw}/N_s is slowed down with increasing the concentration. To further prove this interpretation, the results of W_{bw}/W_w as a function of mole fraction are shown in Figure 6.

The results presented in Figure 6 reveal that W_{bw}/W_w increases with increasing the concentration. It is illustrated that at high concentration, the mass fraction of the “bound water” in total mass of water has less dependence on the concentration than that at low concentration. In detail, the values of W_{bw}/W_w in the MET, EG and GLY solutions increase by the range of 0.81-0.95, 0.88-0.97 and 0.91-0.97 with the concentration increases from 60 to 90 mol %, respectively. When the concentration increases from 1 to 20 mol %, the increasing ranges of W_{bw}/W_w in the three alcohol solutions are 0.02-0.36, 0.030-0.51 and 0.050-0.60, respec-

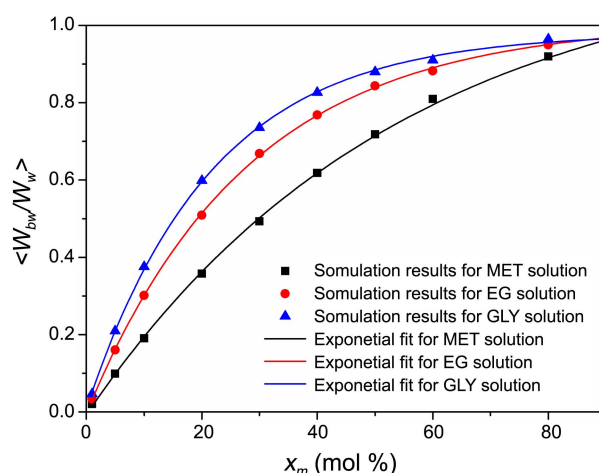


Figure 6. Mass fraction of “Bound water” in total mass of water W_{bw}/W_w as a functions of the concentrations of MET, EG and GLY. W_{bw} is the mass of the “bound water”, and W_w is the total mass of water in the aqueous solution.

Table 2. Values of the fitting parameters a , b and c for the exponential function and the corresponding goodness of fit R^2

	MET solution	EG solution	GLY solution
a	-1.1957	-1.0123	-0.9732
b	0.5398	0.2787	0.2156
c	1.1879	1.0079	0.9804
R^2	0.9993	0.9998	0.9996

tively, which are greater than that at high concentration. Therefore, it is confirmed that the contribution of the added alcohol molecules to the formation of the W-S H-bonds decreases with increasing the concentration.

As shown in Figures 5 and 6, the values of N_{bw}/N_s and W_{bw}/W_w in the aqueous solution of GLY are always larger than those in the MET and EG solutions at a given mole fraction. As stated above, the hydroxyl group content results in that GLY can H-bond more water molecules than MET and EG. Besides, as the concentration increases, the differences of N_{bw}/N_s and W_{bw}/W_w between the three alcohol solutions gradually diminish due to the fact that the proportion of water in the binary mixture becomes smaller and smaller. For quantitative analysis, we employ an exponential decay expression, which was used in our recent experimental study.⁴⁹ The exponential fit for W_{bw}/W_w of the aqueous solutions is depicted in Figure 6, and the fitting parameters a , b and c in Eq. (1) are listed in Table 2.

$$W_{bw}/W_w = a \cdot \exp\left(-\frac{x}{b}\right) + c \quad (1)$$

Contribution of MET, EG and GLY to “Bound Water”.

It has been found that the abilities of MET, EG and GLY hydrogen bonding to water are different as stated above. At appropriate concentrations, the three alcohols could produce the same value of W_{bw}/W_w . To produce the same W_{bw}/W_w for MET and EG, the following equation should be hold,

$$a_m \cdot \exp\left(-\frac{x_m}{b_m}\right) + c_m = a_e \cdot \exp\left(-\frac{x_e}{b_e}\right) + c_e \quad (2)$$

where x_m and x_e are the mole fractions of the MET and EG aqueous solutions, respectively, and a_m , b_m , c_m and a_e , b_e , c_e are the corresponding parameters in Eq. (1) for MET and EG aqueous solutions, respectively.

The practical relationship between x_m and x_e is then obtained from Eq. (2) as below,

$$x_e = b_e \cdot \ln\left(A_1 \cdot \exp\left(-\frac{x_m}{b_m}\right) + B_1\right) \quad (3)$$

where, the introduced parameters A_1 and B_1 are the substitutes for a_m/a_e and $(c_m - c_e)/a_e$, respectively. Similarly, the practical relationship between x_m and x_g can be written as below,

$$x_g = -b_g \cdot \ln\left(A_2 \cdot \exp\left(-\frac{x_m}{b_m}\right) + B_2\right) \quad (4)$$

where, the parameters A_2 and B_2 are the substitutes for a_m/a_g and $(c_m - c_g)/a_g$, respectively.

For ideal case, it is assumed that the H-bonding abilities of each hydroxyl group of MET, EG and GLY in water are identical. This means that equal amount of hydroxyl groups should produce the same W_{bw}/W_w . Taking the aqueous solutions of MET and EG for example, in order to produce equal molar fraction of hydroxyl groups, following relationship should be satisfied,

$$\frac{n_{OH}^e}{n_{OH}^e + n_W^e} = \frac{n_{OH}^m}{n_{OH}^m + n_W^m} \quad (5)$$

where, n_{OH}^e and n_{OH}^m are the numbers of hydroxyl groups in the aqueous solutions of EG and MET, respectively; n_W^e and n_W^m are the numbers of water molecules. The amount of hydroxyl groups is dependent on the quantity of alcohol molecules. For MET aqueous solution, n_{OH}^m equals the number of MET molecules due to the monohydric structure, n_m ; as for EG aqueous solution, n_{OH}^e is twice as the number of EG molecules, n_e . Thus, the following expression is obtained,

$$\frac{2n_e}{2n_e + n_W^e} = \frac{n_m}{n_m + n_W^m} \quad (6)$$

Then the relationship between the mole fractions of x_m and x_e is written as follows,

$$x_e = \frac{x_m}{2 - x_m} \quad (7)$$

Along the same lines, the ideal relationship between x_m and x_g is written as follows,

$$x_g = \frac{x_m}{3 - 2x_m} \quad (8)$$

The practical and ideal relationships between MET and EG, GLY are presented in Figures 7 and 8. It is shown that the practical results are slightly larger than the ideal results,

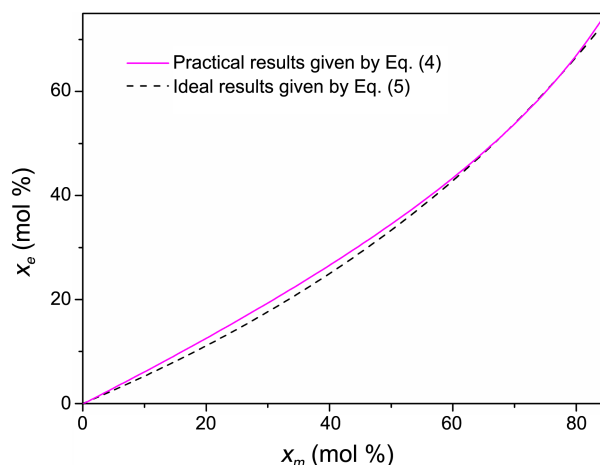


Figure 7. Practical and ideal relationships between x_m and x_e to produce the equal "bound water" fraction W_{bw}/W_w .

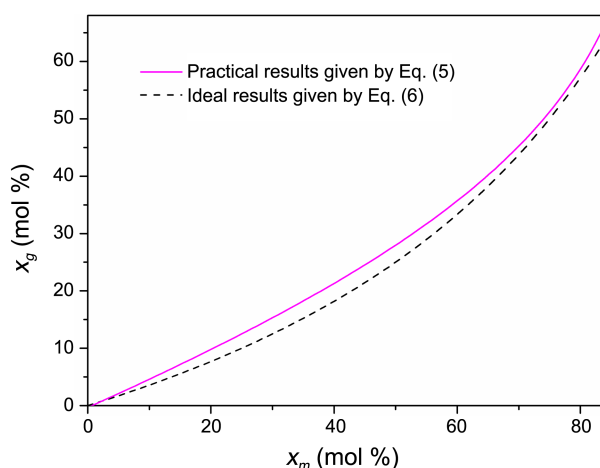


Figure 8. Practical and ideal relationships between x_m and x_g to produce the equal "bound water" fraction W_{bw}/W_w .

that means more hydroxyl groups are needed for EG and GLY to produce the value of W_{bw}/W_w as same as that produced by MET. Moreover, the phenomenon of the larger value for the practical case confirms the results in Figure 2 that the hydroxyl group in the MET molecule favors to form more H-bonds with water than EG and GLY molecules. The practical result in Figure 7 is closer to the ideal results comparing with Figure 8. The comparison proves that the hydroxyl group of EG molecule has greater ability to H-bond water molecules than GLY. As stated in our previous paper,²² the difference between the practical and ideal relationships is due to the intra- and intermolecular interactions of the solute molecules in the MET, EG and GLY aqueous solutions.

H-bonding Lifetime between "Bound water" and Alcohols.

One H-bond will not last until some moment, and then the broken H-bond may reform or disappear. This is due to the fact that the hydrogen bonded molecules have fast librational and vibrational motions in short time intervals. To characterize the dynamics of H-bonding between "bound water" and alcohols, the H-bond time correlation function has been

Table 3. Lifetimes τ_{ws} of the H-bonds between “bound water” and solute in the aqueous solutions of MET, EG and GLY

τ_{ws} (ps) solute	x_s									
	0.01	0.05	0.10	0.20	0.30	0.40	0.50	0.60	0.80	0.90
MET	0.306	0.331	0.361	0.415	0.467	0.531	0.578	0.645	0.792	0.803
EG	0.326	0.340	0.373	0.432	0.492	0.550	0.623	0.682	0.767	0.798
GLY	0.304	0.327	0.354	0.418	0.473	0.527	0.586	0.637	0.689	0.756

calculated. The correlation function for the hydrogen bonded pair i and j is defined as

$$C(t) = \langle h_{ij}(t) \cdot h_{ij}(0) \rangle / \langle h_{ij}(0)^2 \rangle \quad (9)$$

where $h_{ij}(t)$ is an instantaneous population of H-bonds with respect to time. If the molecules i and j are hydrogen bonded at time t , the variable $h_{ij}(t)$ takes the value of 1; otherwise, the variable $h_{ij}(t)$ takes the value of 0. Here, continuous autocorrelation function is chosen to estimate the H-bonding lifetime. This means that one H-bond between two molecules i and j is continuously unbroken from time $t = 0$ to time t is recorded; once it is broken at some point, the H-bond will not be taken into account.

The average H-bonding lifetime (τ_{HB}) is calculated based on the time integral of $C(t)$,⁵⁰

$$\tau_{HB} = \int_0^{\infty} C(t) dt \quad (10)$$

The results of the lifetime of the H-bonds between “bound water” and alcohols are estimated by Eq. (10) and summarized in Table 3. It is shown that the lifetime τ_{ws} increases with increasing the concentration of alcohols. This means that the addition of alcohols will enhance the inhibition to the motion of “bound water”. In the water-rich mixtures, the lifetime τ_{ws} in EG solution is greater than that in MET and GLY solutions with equal molar fraction. This indicates that the middle hydroxyl group of GLY molecule affects the hydrogen bonding interaction with water, as shown in Figure 2. As in the solute-rich mixtures, the lifetime τ_{ws} in MET solution seems longer than the other two solutions. The distinction of the lifetime τ_{ws} should be an origin of the the difference between practical and ideal results depicted in Figures 7 and 8.

Conclusion

In this work, a series of MD simulations have been conducted to investigate the densities and the H-bonding characteristic of the aqueous solutions at different concentrations of CPA solutes involving MET, EG and GLY. According to the simulation results, it can be concluded that the density of the alcohol aqueous solution increases as the concentration increases. Besides, the H-bonding ability of the hydroxyl group of the alcohol molecule decreases with increasing the concentration. Due to the intra-and intermolecular effects, the hydroxyl group of MET has greater H-bonding ability than EG and GLY. However, the H-bonding abilities of EG and GLY molecules are greater than that of MET molecule.

GLY molecule is more active than MET and EG molecules to form H-bond with water molecules due to its high content of hydroxyl groups. With the concentration increases, N_{bw}/N_s decreases and W_{bw}/W_w increases, respectively, consistent with our previous study.²² To obtain certain amount of “bound water”, the use of MET, EG and GLY do not obey the ideal relationship. This should be partly influenced by the hydrogen H-bonding lifetime τ_{ws} between “bound water” and alcohols.

Research on CPA aqueous solution is the solid basis of the comprehensive research of the organic cryopreservation, which has a long way to go. This study offers an insight into the mechanism of the interaction between water and alcohol molecules. To further verify this understanding, it is necessary to implement experimental research like our previous study²³ using DSC method. This will lead the investigation on identifying an optimal practical application of alcohols for cryopreservation.

Supplementary Data. The concentrations and the simulation densities of the EG and GLY aqueous solutions are listed in Table S1(a) and (b), respectively. The time evolution of the total energy, potential energy and kinetic energy of the 90 mol % GLY aqueous solution are shown in Figures S1(a), (b) and (c).

Acknowledgments. The support from the National Nature Science Foundation of China (50976017) and NSFC's Key Program Projects (50736001) is greatly appreciated. And the publication cost of this paper was supported by the Korean Chemical Society.

References

- Dudzinski, D. M. *J. Pediatr. Adolesc. Gynecol.* **2004**, 17(2), 97-102.
- Cañavate, J. P.; Lubiñ, L. M. *Aquaculture* **1995**, 136(3-4), 277-290.
- He, Z.; Liu, H.-C.; Rosenwaks, Z. *Fertil. Steril.* **2003**, 79(2), 347-354.
- Mazur, P. *J. Gen. Physiol.* **1963**, 47, 347-369.
- Jacobs, M. H. *J. Cell Comp. Physiol.* **1933**, 2(4), 427-444.
- Kedem, O.; Katchalsky, A. *Biochim. Biophys. Acta* **1958**, 27, 229-246.
- Chen, H. H.; Purttman, J. J. P.; Heimfeld, S.; Folch, A.; Gao, D. *Cryobiology* **2007**, 55(3), 200-209.
- Karlsson, J. O. M.; Cravalho, E. G.; Toner, M. *J. Appl. Phys.* **1994**, 75(9), 4442-4455.
- Karlsson, J. O. M.; Toner, M. *Biomaterials* **1996**, 17(3), 243-256.
- Toner, M.; Cravalho, E. G. *J. Appl. Phys.* **1990**, 67(3), 1582-1593.
- Toner, M.; Cravalho, E. G.; Karel, M.; Armant, D. R. *Cryobiology*

- 1991, 28(1), 55-71.
12. Storey, K. B.; Baust, J. G.; Buescher, P. *Cryobiology* **1981**, 18(3), 315-321.
13. Li, S.; Dickinson, L. C.; Chinachoti, P. *J. Agr. Food Chem.* **1998**, 46(1), 62-71.
14. Franks, F. *Cryobiology* **1983**, 20(3), 335-345.
15. Lovelock, J. E. *Biochem. J.* **1954**, 56(2), 265-270.
16. Zdenek, H. *Cryobiology* **2003**, 46(3), 205-229.
17. Towey, J. J.; Soper, A. K.; Dougan, L. *Phys. Chem. Chem. Phys.* **2011**, 13(20), 9397-9406.
18. Kyrychenko, A.; Dyubko, T. S. *Biophys. Chem.* **2008**, 136(1), 23-31.
19. Dashnau, J. L.; Nucci, N. V.; Sharp, K. A.; Vanderkooi, J. M. *J. Phys. Chem. B* **2006**, 110(27), 13670-13677.
20. Chen, C.; Li, W. Z.; Song, Y. C.; Yang, J. *J. Mol. Liq.* **2009**, 146(1-2), 23-28.
21. Chen, C.; Li, W. Z.; Song, Y. C.; Yang, J. *J. Mol. Struct-theochem.* **2009**, 916(1-3), 37-46.
22. Weng, L.; Chen, C.; Zuo, J.; Li, W. *J. Phys. Chem. A* **2011**, 115(18), 4729-4737.
23. Weng, L.; Li, W.; Zuo, J.; Chen, C. *J. Chem. Eng. Data* **2011**, 56(7), 3175-3182.
24. Tu, Y.; Fang, H. *Phys. Rev. E* **2009**, 79(1), 016707.
25. Padró, J. A.; Saiz, L.; Guàrdia, E. *J. Mol. Struct.* **1997**, 416(1-3), 243-248.
26. Chen, C.; Li, W.; Song, Y.; Yang, J. *J. Mol. Phys.* **2009**, 107(7), 673-684.
27. Chen, C.; Li, W.-Z. *Acta Phys. -Chim. Sin.* **2009**, 25(3), 507.
28. Phillips, J. C.; Braun, R.; Wang, W.; Gumbart, J.; Tajkhorshid, E.; Villa, E.; Chipot, C.; Skeel, R. D.; Kalé, L.; Schulten, K. *J. Comput. Chem.* **2005**, 26(16), 1781-1802.
29. Jorgensen, W. L.; Chandrasekhar, J.; Madura, J. D.; Impey, R. W.; Klein, M. L. *J. Chem. Phys.* **1983**, 79(2), 926-935.
30. MacKerell, A. D.; Bashford, D.; Bellott, Dunbrack, R. L.; Evanseck, J. D.; Field, M. J.; Fischer, S.; Gao, J.; Guo, H.; Ha, S.; Joseph-McCarthy, D.; Kuchnir, L.; Kuczera, K.; Lau, F. T. K.; Mattos, C.; Michnick, S.; Ngo, T.; Nguyen, D. T.; Prodhom, B.; Reiher, W. E.; Roux, B.; Schlenkrich, M.; Smith, J. C.; Stote, R.; Straub, J.; Watanabe, M.; Wiórkiewicz-Kuczera, J.; Yin, D.; Karplus, M. *J. Phys. Chem. B* **1998**, 102(18), 3586-3616.
31. Reiling, S.; Schlenkrich, M.; Brickmann, J. *J. Comput. Chem.* **1996**, 17(4), 450-468.
32. Martyna, G. J.; Tobias, D. J.; Klein, M. L. *J. Chem. Phys.* **1994**, 101(5), 4177-4189.
33. Darden, T.; York, D.; Pedersen, L. *J. Chem. Phys.* **1993**, 98(12), 10089-10092.
34. Ryckaert, J.-P.; Ciccotti, G.; Berendsen, H. J. C. *J. Comput. Phys.* **1977**, 23(3), 327-341.
35. Sarkisov, G. N.; Dashevsky, V. G.; Malenkov, G. G. *Mol. Phys.* **1974**, 27(5), 1249-1269.
36. Stillinger, F. H.; Rahman, A. *J. Chem. Phys.* **1972**, 57(3), 1281-1292.
37. Loof, H. D.; Nilsson, L.; Rigler, R. *J. Am. Chem. Soc.* **1992**, 114, 4028-4035.
38. Luzar, A.; Chandler, D. *Phys. Rev. Lett.* **1996**, 76(6), 928.
39. Luzar, A.; Chandler, D. *Nature* **1996**, 379(6560), 55-57.
40. Noskov, S. Y.; Lamoureux, G.; Roux, B. *J. Phys. Chem. B* **2005**, 109(14), 6705-6713.
41. Jedlovszky, P.; Turi, L. *J. Phys. Chem. B* **1997**, 101(27), 5429-5436.
42. Marques, M. P. M.; Amorim da Costa, A. M.; Ribeiro-Claro, P. J. A. *J. Phys. Chem. A* **2001**, 105(21), 5292-5297.
43. Zhang, R.; Li, H.; Lei, Y.; Han, S. *J. Phys. Chem. B* **2005**, 109(15), 7482-7487.
44. Dougan, L.; Bates, S. P.; Hargreaves, R.; Fox, J. P.; Crain, J.; Finney, J. L.; Reat, V.; Soper, A. K. *J. Chem. Phys.* **2004**, 121(13), 6456-6462.
45. Towey, J. J.; Soper, A. K.; Dougan, L. *J. Phys. Chem. B* **2011**, 115(24), 7799-7807.
46. Guàrdia, E.; Martí, J.; García-Tarrés, L.; Laria, D. *J. Mol. Liq.* **2005**, 117(1-3), 63-67.
47. Washburn, E. W. (Knovel, U.S., 2003).
48. Guardia, E.; Martí, J.; Padro, J. A.; Saiz, L.; Komolkin, A. V. *J. Mol. Liq.* **2002**, 96-97, 3-17.
49. Weng, L.; Li, W.; Zuo, J. *Cryobiology* **2011**, 62(3), 210-217.
50. Elola, M. D.; Ladanyi, B. M. *J. Chem. Phys.* **2006**, 125, 184506.
51. Iulian, O.; Ciocîrlan, O. *Rev. Roum. Chim.* **2010**, 55, 45-53.